

UNIVERSITÉ CATHOLIQUE DE LOUVAIN

**Study of the stress relieve heat-treatment of
additively manufactured AlSi10Mg alloy:**
Influence on microstructure and mechanical properties

Dissertation presented by

David DISPAS

and

Arthur BOUILLOT

for obtaining the Master's degree in

Mechanical Engineering

and

Chemical and Materials
Engineering

at Ecole Polytechnique de Louvain (EPL)

Supervisor: Aude SIMAR

Readers: Laurent DELANNAY, Anne MERTENS, Camille VAN DER REST

Academic year 2017-2018

'Citation stylée.'

Mec cool

Acknowledgements

Gros betch à mes poules Aude Simar et Camille Van Der Rest et aux potos du labo

Contents

1	Introduction	1
2	State of the art	3
3	Materials and methods	9
4	Results	11
5	Discussion	13
6	Conclusion	15
	Bibliography	17

List of Figures

2.1	Selective laser melting technology principle	3
2.2	(a)Research publications on SLM of all materials, ceramics and composite. (b)Research publications on SLM of different metallic materials. Data are derived from the research publications on SLM, Laser-Cusing and DMLS existing on <i>ScienceDirect</i>	4
2.3	Parameters involved in SLM	4
2.4	Process window for SLM of AlSi10Mg, based on the top view of single track scans	5
2.5	Process window for SLM of AlSi10Mg, based on the front view of single track scans	6
2.6	Schematic representation of scanning strategies commonly used in LSM (a) unidirectional long scan track; (b) bi-directional long scan track, and (c) islands	6
2.7	Samples (static tensile) built in different directions: (a) 0°, (b) 45°, and (c) 90°	7
5.1	An Electron	13

List of Tables

List of Abbreviations

CAD	Computer Aided Design
DMLS	Direct Metal Laser Sintering
SLM	Selective Laser Melting

Symbols

D_a	Average particle size	$[\mu m]$
E_d	Volumetric energy density	$[\frac{J}{mm^3}]$
h	Hatch space	$[\mu m]$
P	Laser power	$[W]$
p_{O_2}	Oxygen pressure	$[mbar]$
t	Layer thickness	$[\mu m]$
v_s	Scanning speed	$[\frac{mm}{s}]$
$\phi_{99\%}$	Laser spot size at the 99% contour	$[\mu m]$
ρ_{rel}	Apparent relative density	$[-]$

Nous dédions ce travail à nos familles et amis

Chapter 1

Introduction

This is, with the concluding chapter, a significant portion of memory. This should especially present the context and objectives of the work. Generally, the memory structure (content of chapters) is briefly exposed

Chapter 2

State of the art

Selective laser melting (SLM) - also referred to as direct metal laser sintering (DMLS) - is an additive manufacturing technique making use of a high power-density laser to locally melt layers of powder materials. Layers are progressively piled up, in order to create a 3D part. The technique is illustrated on figure 2.1 [7]. The materials used include mostly metals but also ceramics and composites. Parts to build must first be drawn in a computer-aided design (CAD) software and broke down in 2D slices, each one corresponding to a powder layer. During the process, the oxygen pressure p_{O_2} must be kept low to prevent the oxidation of the metal. A shielding gas - such as argon - is thus used to fill the build chamber and p_{O_2} must be monitored at all time.

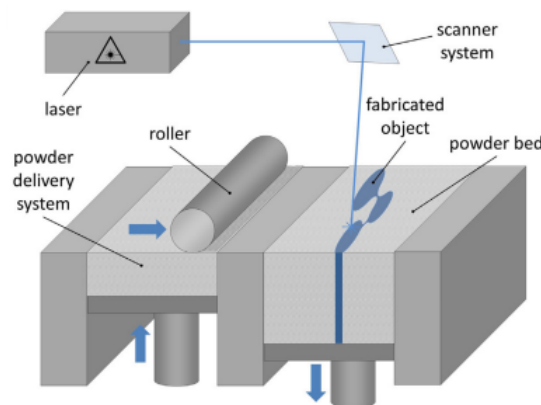


FIGURE 2.1: Selective laser melting technology principle (from Leitz et al, 2016).

LSM is still a young technology. Its popularity only increased significantly over the last few years, as depicted by figures 2.2 (a) and (b). Works concerning AlSi10Mg began to emerge noticeably in 2014. Applications for the technique are many: biomedical, heat exchangers, aerospace and automotive - to name just a few [14]. The main appeals of LSM

Parler de l'AlSi10Mg; quel est l'intérêt de travailler avec? Difficultés? (reflectivité etc)

Microstructure homogène, diagramme de phase

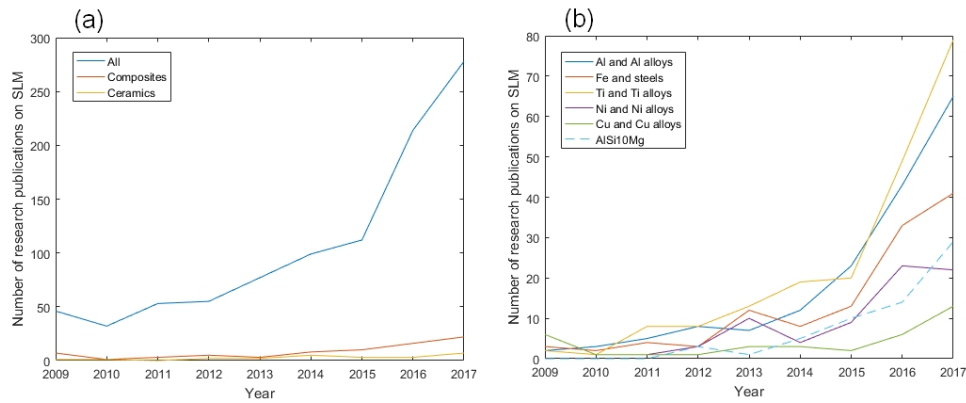


FIGURE 2.2: (a) Research publications on SLM of all materials, ceramics and composite. (b) Research publications on SLM of different metallic materials. Data are derived from the research publications on SLM, LaserCusing and DMLS existing on ScienceDirect website.

The properties of parts produced through SLM stem from the coupled effects of a great deal of parameters (see figure 2.3) [2]. Results are very sensitive to their variations. The process parameters must thus be monitored thoroughly. This complicates the search for their optimisation, still not fully resolved for aluminium alloys.

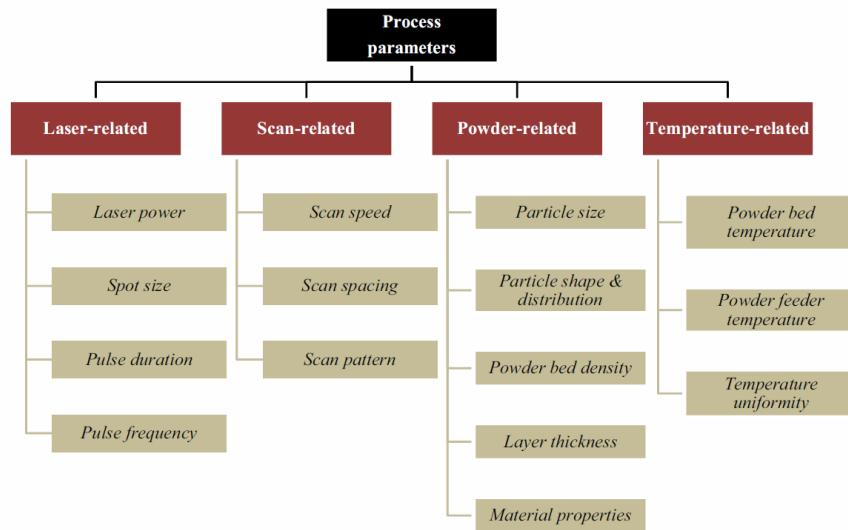


FIGURE 2.3: Parameters involved in SLM (from Aboulkhair et al, 2014).

In recent years, works aiming at facing this challenge multiplied. The minimisation of the porosity is at the center of attention. It is indeed closely related to the quality of the mechanical properties. As porosity contributes to lowering the load-bearing surface, it reduces the apparent material strength. It was also observed to have a critical influence on the fatigue life of the produced parts. Their lifetime is especially diminished if the values of pores amount and size go beyond a certain threshold [4]. Studies investigating the effects of various parameters on the

AlSi10Mg fabrication through SLM abound in the literature.

The analysis of the paired impacts of the laser power P and scan speed v_s provides a first insight. As depicted by figures 2.4 and 2.5, low P and high v_s lead to an insufficient energy input to melt the powder and re-melt the substrate, which causes the formation of droplets [6]. The opposite leads to good penetration but also to distortions and irregularities. A trend to use both high P and v_s rose in accordance with these findings. Doing so has the advantage to increase productivity. However, it also has multiple downsides including a decrease of the surface quality due to balling, excessive spatter, and an augmented gas induced porosity [9]. Therefore, a trade-off must be found.

A popular approach is to regroup multiple operating parameters into one, the volumetric energy density E_d . It is estimated through the following formula:

$$E_d = \frac{P}{v_s h t}$$

where t is the layer thickness and h is the hatch space. As a rule of thumb, E_d should be chosen in the range between 60 and 75 [$\frac{J}{mm^3}$] [11]. However, the criterion is insufficient and others should be considered such as melt pools overlapping [12]. Almost no studies were carried out to optimize h and t independently. Their values lie generally respectively in the intervals [20 ; 60] [μm] and [50 ; 200] [μm].

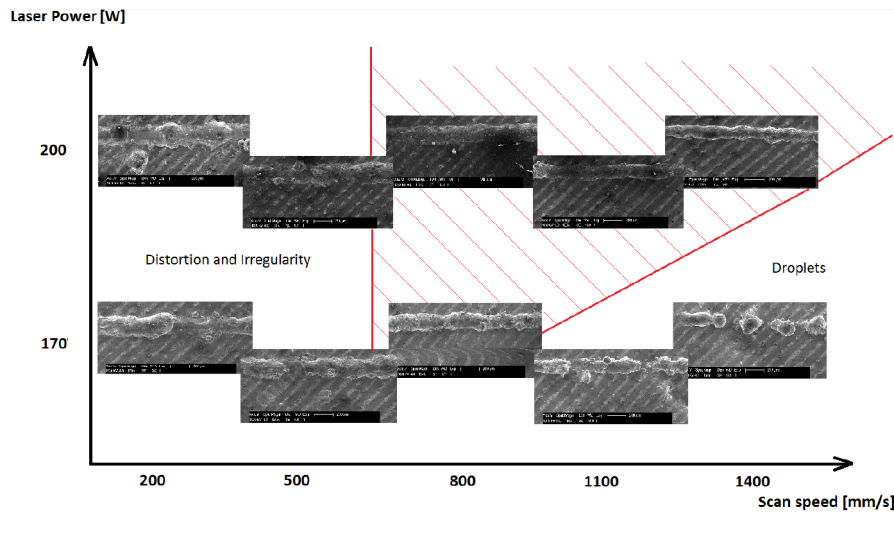


FIGURE 2.4: Process window for SLM of AlSi10Mg, based on the top view of single track scans (from Kempen et al, 2011).

The other process parameters will be covered for the sake of completeness. Let us first look into the particle-related parameters. The particle size D_a of the powder should be as small as possible to ensure a good flowability and allow for thin layers [6]. Typical values stretch from 15 to 60 [μm]. The size distribution is more delicate to outline. On one hand, wider distributions often generate better bed density, parts with higher density and better surface finish. On the other hand, narrower ones usually provide better flowability and parts with better strength and hardness [8]. In most cases, a middle ground between the two should be sought. In SLM

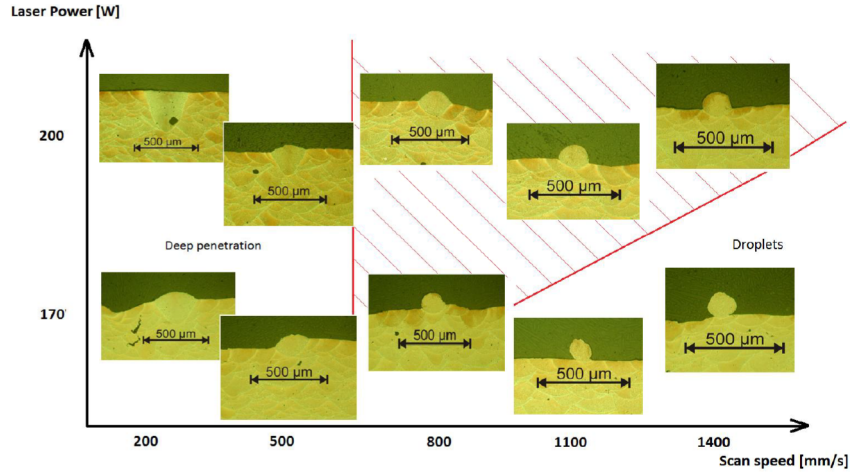


FIGURE 2.5: Process window for SLM of AlSi10Mg, based on the front view of single track scans (from Kempen et al, 2011).

applications, powder is often successively recycled multiple times. This leads to their progressive contamination with moisture, which causes an increase of hydrogen porosity in the produced parts [13]. The problem can be overcome by drying the powder or using fresh one. Unfortunately - in the case of aluminium alloys - no findings were made regarding the prediction of a threshold at which one should take action [3].

The choice of scan pattern has great importance. There exist a few strategies. The common ones use unidirectional, bidirectional or islands patterns (see figure 2.6). The scan direction(s) should be rotated between successive layers to favorise isotropy, especially in the unidirectional case since it causes height variations along a layer [1]. The islands pattern is based on a decomposition in small domains with short scanning tracks. Two usual strategies can be distinguished among this group: the chessboard and the hexagonal one.

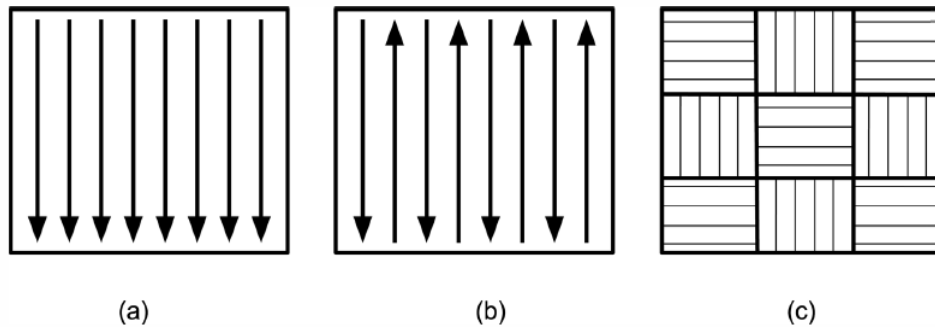


FIGURE 2.6: Schematic representation of scanning strategies commonly used in LSM (a) unidirectional long scan track; (b) bidirectional long scan track, and (c) islands (from Mertens et al, 2017).

Furthermore, dual scanning strategies were proven to be effective. For example, a pre-scan with low E_d can flatten the powder bed before it is consolidated, which

leads to a reduction of porosity [9]. It was also shown that scanning the contour of the part being built at lower E_d can better the surface roughness for AlSi12Mg [10]. One should note too that the final properties of the fabricated part can strongly depend on the building direction (see figure 2.7) [5].

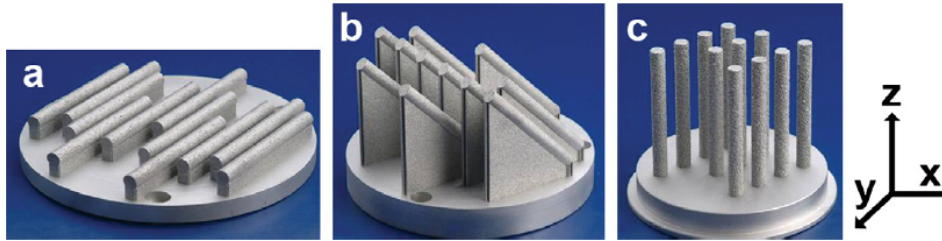


FIGURE 2.7: Samples (static tensile) built in different directions: (a) 0° , (b) 45° , and (c) 90° (from Brandl et al, 2012).

Other laser-related parameters - the spot size and the pulse properties - can also influence the process. Only the laser spot size at the 99% contour $\phi_{99\%}$ is frequently cited in literature. Its value lies between 100 and 200 $[\mu m]$.

Finally, the temperature of the powder bed and feeder affect the final properties of the fabricated parts as well. In particular, it was observed that pre-heating the powder at $300^\circ C$ mitigates the differences of fatigue resistance between tensile specimens built in different directions: it is possible that the slower cooling rate induced helps reducing the distortions and internal stresses [4].

Comparer les résultats avec alliage coulé/forgé

Once the porosity problem is sorted out, other matters can be addressed such as productivity and surface roughness. The latter is problematic as the surface finish obtained with SLM is typically of such poor quality that all cracks initiate near the surface for a sample with apparent relative density $\rho_{rel} > 99\%$ [4]. Polir ou changement paramètres fab.

Post-traitements dont traitements thermiques, sur lesquels on se focalise. Expliquer

Chapter 3

Materials and methods

Description expériences et machines

Chapter 4

Results

Analyses statistiques etc...

Chapter 5

Discussion

Que conclure d'après les résultats? 5.1



FIGURE 5.1: An electron (artist's impression).

Chapter 6

Conclusion

They incorporate in a synthetic way the main results and compare them with the initial objectives. Generally, this final chapter also presents prospects for the continuation of the work undertaken.

Bibliography

- [1] Nesma T. Aboulkhair et al. 'On the formation of AlSi10Mg single tracks and layers in selective laser melting: Microstructure and nano-mechanical properties'. In: *Journal of Materials Processing Tech.* 230.Complete (2016), pp. 88–98.
- [2] Nesma T. Aboulkhair et al. 'Reducing porosity in AlSi10Mg parts processed by selective laser melting'. In: *Additive Manufacturing* 1-4 (2014). Inaugural Issue, pp. 77 –86. URL: <http://www.sciencedirect.com/science/article/pii/S2214860414000062>.
- [3] Nesma T. Aboulkhair et al. 'Selective laser melting of aluminum alloys'. In: *MRS Bulletin* 42.4 (2017), 311–319.
- [4] Erhard Brandl et al. 'Additive manufactured AlSi10Mg samples using Selective Laser Melting (SLM): Microstructure, high cycle fatigue, and fracture behavior'. In: *Materials & Design* 34 (2012), pp. 159 –169. URL: <http://www.sciencedirect.com/science/article/pii/S0261306911005590>.
- [5] Pauline Delroisse et al. 'Effect of strut orientation on the microstructure heterogeneities in AlSi10Mg lattices processed by selective laser melting'. In: *Scripta Materialia* 141 (2017), pp. 32 –35. ISSN: 1359-6462.
- [6] Karolien Kempen et al. 'Microstructural analysis and process optimization for selective laser melting of AlSi10Mg'. In: *Solid Freeform Fabrication Symposium Proceedings* (2011). Conference paper, pp. 484–495. URL: <https://sffsymposium.engr.utexas.edu/Manuscripts/2011/2011-37-Kempen.pdf>.
- [7] K.-H. Leitz et al. 'Multi-physical simulation of selective laser melting'. In: *Metal Powder Report* 72.5 (2017), pp. 331 –338. URL: <http://www.sciencedirect.com/science/article/pii/S0026065716300200>.
- [8] Bochuan Liu et al. 'Investigaztion the effect of particle size distribution on processing parameters optimisation in selective laser melting process'. In: (Jan. 2011). Conference paper, pp. 227–238.
- [9] Anne I. Mertens, Jocelyn Delahaye and Jacqueline Lecomte-Beckers. 'Fusion-Based Additive Manufacturing for Processing Aluminum Alloys: State-of-the-Art and Challenges'. In: *Advanced Engineering Materials* 19.8 (2017), p. 1700003. URL: <https://onlinelibrary.wiley.com/doi/abs/10.1002/adem.201700003>.
- [10] K.G. Prashanth, S. Scudino and J. Eckert. 'Defining the tensile properties of Al-12Si parts produced by selective laser melting'. In: *Acta Materialia* 126 (2017), pp. 25 –35. URL: <http://www.sciencedirect.com/science/article/pii/S135964541630982X>.
- [11] Noriko Read et al. 'Selective laser melting of AlSi10Mg alloy: Process optimisation and mechanical properties development'. In: *Materials & Design* (1980-2015) 65 (2015), pp. 417 –424. URL: <http://www.sciencedirect.com/science/article/pii/S0261306914007468>.

- [12] Ming Tang, P. Chris Pistorius and Jack L. Beuth. 'Prediction of lack-of-fusion porosity for powder bed fusion'. In: *Additive Manufacturing* 14 (2017), pp. 39 – 48. URL: <http://www.sciencedirect.com/science/article/pii/S2214860416300471>.
- [13] Christian Weingarten et al. 'Formation and reduction of hydrogen porosity during selective laser melting of AlSi10Mg'. In: *Journal of Materials Processing Technology* 221 (2015), pp. 112 –120. URL: <http://www.sciencedirect.com/science/article/pii/S0924013615000564>.
- [14] Chor Yen Yap et al. 'Review of selective laser melting: Materials and applications'. In: 2 (Dec. 2015), p. 041101.